

# Electrical contact resistance measurements of clamped battery cell connectors for cylindrical 18650 battery cells



Christoph Bolsinger\*, Matthias Zorn, Kai Peter Birke

Department of Electrical Energy Storage Systems, Institute for Photovoltaics, University of Stuttgart, 70569 Stuttgart, Germany

## ARTICLE INFO

### Article history:

Received 15 September 2016  
Received in revised form 5 April 2017  
Accepted 6 April 2017  
Available online 13 April 2017

### Keywords:

Disassemble and recycling concepts  
Future battery module architectures  
Battery cell connectors  
Electrical contact resistance  
Clamped cell connector  
Battery assemblies

## ABSTRACT

The present study investigates the application of clamped cell connectors for 18650 battery cells with focus on the electrical contact resistance (ECR). The ECR, which occurs at the contact interface, is one of the crucial criterion to design a battery cell joint. A poor connection with an increased contact resistance can lead to a significant heat generation and can subsequently cause a heat transfer into the battery cell. A positive terminal of a Panasonic NCR18650B Li-Ion cell is used for ECR measurements and for an investigation of the mechanical properties. A load test indicates that the positive terminal undergoes an elastic deformation up to a force of about 400 N and can therefore be used for clamped joints without any damage. To investigate the dependencies of ECR, the applied force on the joint is varied from 25 to 400 N and five different materials with three different surface roughnesses are used as cell connectors. Furthermore, the influence of aged surfaces is investigated. The obtained data show that the ECR of clamped cell connectors is reduced to about  $50 \mu\Omega$ . Thus, the ECR is in the range or even lower than for welded contacts.

© 2017 Elsevier Ltd. All rights reserved.

## 1. Introduction

For large energy storage systems up to several thousand cells have to be assembled and connected (Tesla, Model S). One of the crucial criterion to evaluate a battery cell joint is the electrical contact resistance, which occurs at the contact interface due to the constriction of the electrical current. High electrical contact resistance generates ohmic power loss which leads to a heat generation and subsequently cause a heat transfer into the battery cell. Furthermore, high electrical contact resistance (ECR) reduces the efficiency and the power capability of the battery cells.

Currently welding processes like resistance spot, ultrasonic or laser beam welding are commonly used to interconnect battery cells [1]. Besides the heat input during the welding process a huge drawback of welded battery cell connections is the complex disassembling process whereas the contact elements have to be disrupted from each other. An easy way to assemble and disassemble battery cells without damaging is the use of clamped cell connectors [1]. Therefore, a contact force is applied between the

cell and the cell connector. While clamped cell connections are known for pouch cells [2], whereas the collector bars are attached to the battery electrode tab via brackets, there exists not a similar solution for cylindrical battery cells.

To ensure a good joint, the electrical contact resistance has to be investigated in detail. Taheri, Hsieh and Bahrami measured the electrical contact resistance of clamped cell connectors for a prismatic lithium-ion-polymer battery cell [2]. They show that the ECR can be reduced to a value of about  $10 \text{ m}\Omega$  by applying a sufficient force on the contact. The works of Brand et al. and Schmidt et al., show the measurement of the electrical contact resistance for welded cell connections [3,4]. Laser beam welding achieves the lowest ECR of about  $130 \mu\Omega$ .

This paper investigates the electrical contact resistance of clamped cylindrical battery cells (18650 format). Because of the complex geometry and the limited contact area the measurements are focused on the positive terminal of the cell. A load test of the positive terminal shows the range of elastic deformation. Subsequent measurements identify the most crucial effects on the ECR. Additional measurements with aged surfaces of the contact elements show the effect of a possible film resistance. The experimental results are described by multipoint contact theory.

\* Corresponding author.

E-mail address: [christoph.bolsinger@ipv.uni-stuttgart.de](mailto:christoph.bolsinger@ipv.uni-stuttgart.de) (C. Bolsinger).

## 2. Theoretical background

The ECR depends on oxidation and corrosion, contact load, temperature, and other parameters of a multipoint contact [5–8]. Battery cell connection is usually stationary mechanism and can be divided into non-separable joints (welding, soldering, gluing) and clamped joints (bolted, screwed, wrapped). The contact interface depends on the contact load and the material constants of the contact members. Fig. 1(a) shows the real surface of the contact members consisting of many asperities and the current through the contact interface. Thus, the real conducting contact area  $A_r$  comprises only a small portion of the apparent contact area  $A_a$ . Fig. 1(b) shows the different surface areas of a loaded cell connector. An existing load-bearing area  $A_{lb}$  that is covered by a natural oxide and other contaminant films can electrically isolate the real conducting contact area  $A_r$ .

Hence the current is passing the interface only through the so called a-spots (conducting contact area), an additional constriction resistance  $R_C$  increases the conductor resistance  $R_M$ , which results from electrical resistivities of the materials. The total constriction resistance  $R_C$  is a parallel connection of  $n$  single a-spots  $R_{C,i}$

$$R_C = \left( \sum_{i=1}^n \frac{1}{R_{C,i}} \right)^{-1}. \quad (1)$$

The spreading resistance, which is based on the work made by Maxwell, describes the resistance of a circular single spot  $R_S$  and depends on the specific resistances of the contact members  $\rho_1$  and  $\rho_2$  and the radius of the single a-spot  $a$  [9]:

$$R_S = \frac{\rho_1 + \rho_2}{4a} \quad (2)$$

Based on Eqs. (1) and (2) the constriction resistance  $R_C$  will decrease with increasing number and area of a-spots. Therefore the contact resistance  $R_C$  depends on the surface topology (e.g. surface roughness) and the applied force  $F$ . If the force increases, the conducting contact area will increase due to the disruption of the isolated oxide film and the elastic-plastic deformation of the contact spots. For plastic deformation the applied Force  $F$  is the product of the hardness of the softer contact material  $H$ , the real contact area  $A_r$  and the pressure factor  $\zeta$  [10]

$$F = \zeta H A_r. \quad (3)$$

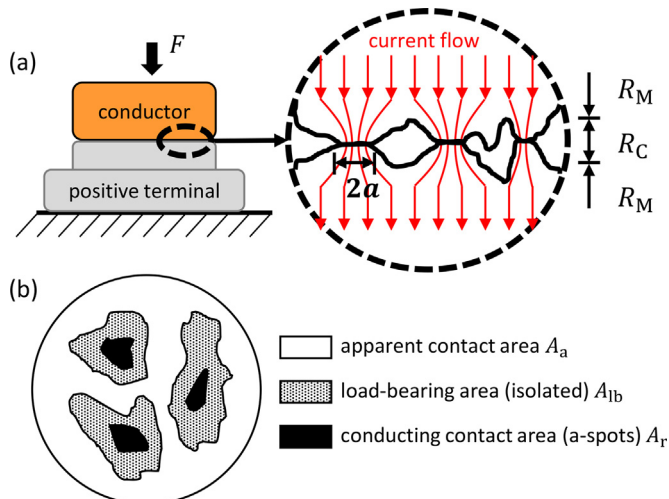


Fig. 1. The contact interface in (a) only exists by some metallic contacts where the current flows through. (b) The different contact areas.

The pressure factor depends on the amount of deformation of the asperities and is equal to one in most practical contact systems. The real area in Eq. (3) also includes the load-bearing area which is covered with an isolated oxide or other surface contaminant films. The additional resistance of the film  $R_f$  can cover the conducting a-spot. The resistance is assumed as a round slice on the conducting spot and depends on the resistivity of the contaminant material  $\rho_c$ , the thickness of the film resistance  $d_c$  and the radius of the single spot  $a$

$$R_f = \frac{\rho_c d_c}{\pi a^2}. \quad (4)$$

The resistance per area  $\sigma = \rho_c d_c$  depends on the applied force  $F$ , the time  $t$  and temperature  $T$ . With Eqs. (2) and (4) the total resistance of a single spot  $R_{C,i}$  is

$$R_{C,i} = R_S + R_f. \quad (5)$$

The spreading resistance (a-spot)  $R_S$  and the applied force can be correlated by inserting Eq. (3) in (2). Therefore  $a = \sqrt{F/\pi H}$  is the radius of the real contact area  $A_r$ . The pressure factor  $\zeta$  is assumed to be one.

$$R_S = \frac{(\rho_1 + \rho_2)\sqrt{\pi H}}{4} F^{-0.5} \quad (6)$$

Inserting Eq. (3) in Eq. (4) gives the correlation between the film resistance  $R_f$  and the applied force  $F$ . Therefore  $a$  is again the radius of the real contact area  $A_r$ .

$$R_f = \frac{\rho_c d_c H}{\pi} F^{-1} \quad (7)$$

The sum of Eqs. (6) and (7) gives the total constriction resistance  $R_C$  as a function of the applied force  $F$ . The factor  $k$  considers the fact that the real contact area  $A_r$  (sum of a-spots) is only a small fraction of the load-bearing area  $A_{lb}$  which depends on the surface roughness.

$$R_C = \frac{(\rho_1 + \rho_2)\sqrt{\pi H}}{4k} F^{-0.5} + \frac{\rho_c d_c H}{\pi k} F^{-1} = r_s F^{-0.5} + r_f F^{-1} \quad (8)$$

The factors  $r_s$  and  $r_f$  simplify the expression. After the factors are fitted to the measurement results in Section 4 they give information about the proportion of the spreading resistance and the film resistance on the total constriction resistance.

## 3. Clamped cell connectors for 18650 battery cells

In common battery assemblies the joint between the battery cell and the current collector (cell connector) is realized by different welding techniques like spot, laser beam or ultrasonic welding. An alternative joint for connecting battery cells is a clamped electrical contact. The advantage of clamped joints compared to non-separable joints is the use of intermediate contact parts which can be assembled and disassembled without damaging the joint. Table 1 lists further benefits and drawbacks of clamped and welded joints [1].

Especially the positive terminal has to be investigated with respect to the mechanical and electrical properties because of the complex geometry and special functions like bursting mechanism. The investigations in this work are exemplary done with a Panasonic NCR18650B Li-Ion cell. Fig. 2(a) shows a detached positive terminal of a NCR18650B battery cell. The diameter of 7 mm which ends up in the mounting ribs defines the maximum possible clamping area. To obtain the material composition, the cross section of the clamping area is analyzed by energy dispersive X-ray spectroscopy (EDX). The EDX shows that the clamping area consists of nickel-plated iron. The nickel layer is about 56  $\mu\text{m}$

Download English Version:

<https://daneshyari.com/en/article/5127284>

Download Persian Version:

<https://daneshyari.com/article/5127284>

[Daneshyari.com](https://daneshyari.com)